

# Maximum Mixing Times of Methane and Air

Dan Brasoveanu\* and Ashwani K. Gupta†  
*University of Maryland, College Park, Maryland 20742*

The combined effect of the distribution of fuel, air, temperature, pressure, and velocity in a combustor on methane–air mixing times is examined using a unified mixing model. The model is designed to study mixing under both nonreacting and reacting conditions up to the flame front at low pressures. The degree and rate of mixing is quantified using the local equivalence ratio and its total derivative with respect to time, respectively. Results show that velocity divergence, and rates of pressure and temperature affects mixing. The model is validated using available experimental results. Two mixing mechanisms that can be distinguished are air penetration into the fuel flow and fuel dispersion into the surrounding air. Algorithms to calculate the rates of mixing and mixing times for both these mechanisms are presented. Results show that under both reacting and nonreacting conditions, the maximum mixing time is directly proportional to the initial pressure and temperature of mixture and inversely proportional to rates of pressure and temperature, and to velocity divergence. Mixing through fuel dispersion into the surrounding air is shown to be faster than via air penetration into the fuel flow. The range of conditions for the distributions of pressure, temperature, and velocity have been chosen to represent characteristic conditions encountered in most low-pressure combustors. Rates of pressure of less than one atm/s acting alone provide a mixing time in excess of one second, which is unacceptably long for many applications, in particular gas turbine combustion. Rates of temperature that act alone may provide mixing times of 0.001 s or less. Mixing times of the order of a few milliseconds, required for efficient combustion and low emission, require high velocity gradient at the fuel–air boundary. Results show that enhanced mixing is achieved by combining temperature and velocity gradients. This analysis of mixing time assists in providing design guidelines for the development of high intensity, high efficiency, and low emission combustors.

## Nomenclature

$dP/dt$	=	rate of pressure, atm/s
$(dP/dt)_{\max}$	=	maximum rate of pressure, atm/s
$(dP/dt)_{\min}$	=	minimum rate of pressure, atm/s
$dT/dt$	=	rate of temperature, K/s
$(dT/dt)_{\max}$	=	maximum of rate of temperature, K/s
$(dT/dt)_{\min}$	=	minimum rate of temperature, K/s
$\text{div } \mathbf{U}$	=	velocity divergence, 1/s
$\text{div } \mathbf{U}_{\max}$	=	maximum velocity divergence, 1/s
$\text{div } \mathbf{U}_{\min}$	=	minimum velocity divergence, 1/s
$\mathbf{e}_1, \mathbf{e}_2, \mathbf{e}_3$	=	unit vectors along the $x, y, z$ axes
$M$	=	molecular weight of mixture, kg/kmol
$M(0)$	=	initial molecular weight of mixture, kg/kmol
$M_a$	=	molecular weight of air, kg/kmol
$M_f$	=	molecular weight of fuel, kg/kmol
$m_a$	=	mass of air, kg
$m_f$	=	mass of fuel, kg
$(m_a/m_f)_{\text{st}}$	=	stoichiometric mass ratio of fuel and air
$P$	=	pressure, atm
$R$	=	universal gas constant/atmospheric pressure, $\text{m}^3/\text{Kmol-K}$
$R_n$	=	fuel nozzle radius, m
$r_e$	=	rate of equivalence ratio, 1/s
$r_e^{\text{(exp)}}$	=	experimental rate of equivalence ratio, 1/s
$r_e^{\text{(max)}}$	=	maximum rate of equivalence ratio, 1/s
$r_e^{\text{(min)}}$	=	minimum rate of equivalence ratio, 1/s
$T$	=	temperature, K
$t$	=	time, s
$t_l$	=	fuel-lean mixing time, s
$t_l^{\text{(max)}}$	=	maximum fuel-lean mixing time, s

$t_r$	=	fuel-rich mixing time, s
$t_r^{\text{(max)}}$	=	maximum fuel-rich mixing time, s
$\mathbf{U}$	=	velocity, m/s
$u$	=	component of velocity along the $x$ direction, m/s
$u_{\text{cyl}}$	=	axial velocity component in cylindrical coordinates, m/s
$v$	=	component of velocity along the $y$ direction, m/s
$w$	=	component of velocity along the $z$ direction, m/s
$x$	=	Cartesian coordinate along the $X$ axis, m
$x_{\text{ax}}$	=	axial cylindrical coordinate, m
$y$	=	Cartesian coordinate along the $Y$ axis, m
$z$	=	Cartesian coordinate along the $Z$ axis, m
$\iota$	=	integration variable, s
$\rho$	=	total density, $\text{kg}/\text{m}^3$
$\rho(0)$	=	initial density, $\text{kg}/\text{m}^3$
$\phi(0)$	=	initial equivalence ratio, dimensionless
$\phi^{\text{(min)}}(t)$	=	minimum equivalence ratio, dimensionless
$\phi(t)$	=	equivalence ratio, dimensionless
$\nabla$	=	del vector operator

## I. Introduction

THE role of a combustor is very important in all systems that convert chemical energy into heat by combustion.<sup>1</sup> The overall efficiency and pollutant's emission level depend on combustor design amongst other parameters. With the limited resources of fossil fuels, efforts must be taken to conserve energy e.g., by enhancing combustion efficiency. Compact combustor designs<sup>2</sup> are desirable as they also help conserve fuel. Increased power output, flame stability and relighting capability and combustor durability are perennial concerns. New combustor designs are required to satisfy continuously increasing stringent environmental regulations.<sup>3,4</sup>

Combustor designs have to accommodate many compromising requirements.<sup>4</sup> As an example, lowering the flame temperature and/or residence time in the combustor reduces  $\text{NO}_x$ . However, higher thermodynamic efficiency requires higher temperatures.<sup>5</sup> Shorter residence time also reduces  $\text{NO}_x$  emission, whereas enhanced mixing and subsequently increased chemical conversion efficiency requires longer residence times.<sup>2,3</sup> Swirl, although very

Received 1 March 1999; accepted for publication 13 January 2000. Copyright © 2000 by Dan Brasoveanu and Ashwani K. Gupta. Published by the American Institute of Aeronautics and Astronautics, Inc., with permission.

\*Research Engineer, The Combustion Laboratory, Department of Mechanical Engineering.

†Professor, The Combustion Laboratory, Department of Mechanical Engineering. Fellow AIAA.

useful for enhancing fuel-air mixing, can cause flame instability and increased NO<sub>2</sub> emission levels.<sup>6</sup> To satisfy such wide design requirements, combustion phenomena must be better understood.<sup>7</sup> A wide variety of complex phenomena in combustion include turbulence, chemical kinetics, mixing, and flow aerodynamics.<sup>8</sup> Improved combustor design requires a better understanding of each phenomenon in part and also their interaction. Chemical reactions cannot proceed until fuel and oxidant are mixed on a molecular level,<sup>9</sup> i.e., the distance between fuel and oxidant molecules is smaller than their mean free path.<sup>1</sup> In addition, the ratio between fuel and air has to lie within the flammability limits.<sup>6</sup> Fuel-air mixing is one of the most important and challenging combustion problems. Mixing affects both combustor efficiency and pollutant's emission.<sup>2</sup>

Combustor performance depends on burner geometry, design and location of air and fuel inlets, fuel type and operational conditions. An effective investigation strategy, based on global combustor design parameters, is effective for determining the role of promising designs prior to performing experiments or full computational fluid dynamics simulations. Analytical models can provide valuable guidelines.<sup>10</sup>

## II. Overview of Mixing Models

Previous studies have often been focused on some specific mixing studies as the mixing phenomenon is considered to be too complicated to allow for the formulation of a general model.<sup>11</sup> Various mixing steps that can be identified include: distributive mixing, dispersive mixing, and diffusive mixing.<sup>12</sup> The distributive mixing is provided by large eddies and yields homogeneity on a large scale. The dispersive mixing is the shearing and breaking of large eddies into a multitude of small size eddies and yields a finer grain mixture. The diffusive mixing is caused by motion of individual molecules. The first two (distributive and dispersive) are also known as mechanical mixing.

Previous models on mixing have attempted to separate the mechanical and diffusive mixing in addition to the chemical kinetics.<sup>11</sup> These models have focused on the kinematics of fluid particles, either by attempting a detailed kinetic study of stretching and folding of fluid surfaces, or by a stochastic analysis of shuffling the given particles.<sup>11</sup> Mixing was treated as a succession of independent steps of a potentially infinite number of steps involving either mechanical or diffusive mixing but not both. To calculate the overall mixing time, mechanical and diffusive mixing times were assumed to be additive. Mixing and intensity of chemical reactions are interdependent.<sup>11</sup> The chemical reaction interaction had to be ignored except in a few particular cases. In spite of all of these simplifying assumptions the kinetic approach of mixing is faced with formidable difficulty when quantitative answers are desired because the motion of fluid particles is chaotic in nature.<sup>13</sup> In summary, mixing studies that focus on the kinematics of fluid particles are very cumbersome and provide only approximate answers to some specific problem. A unified treatment of mechanical and diffusive mixing is lacking.<sup>14</sup>

## III. Theoretical Approach

A unified mixing model has been presented in a previous publication by the authors.<sup>15</sup> The model predictions are compared here with the available experimental results. The methane-air mixing times are also determined.

The degree of mixing attained within an infinitesimal mixture element can be quantified using the local equivalence ratio  $\phi$ . Assuming an ideal gas mixture containing  $n_f$  moles of fuel and  $n_a$  moles of air,<sup>15</sup> the number of moles of fuel and air can be calculated from

$$n_f = m_f / M_f, \quad n_a = m_a / M_a$$

Therefore

$$(\rho_f / M_f) + (\rho_a / M_a) = P / RT$$

where

$$\rho_f + \rho_a = \rho$$

As a consequence, the densities of fuel and air, respectively, can be expressed as

$$\rho_f = [M_f / (M_f - M_a)] [\rho - M_a (P / RT)]$$

$$\rho_a = [M_a / (M_f - M_a)] [M_f (P / RT) - \rho]$$

The correlation between local equivalence ratio, pressure, temperature, and total density is given by<sup>15</sup>

$$\phi = \left( \frac{m_a}{m_f} \right)_{st} \frac{M_f \rho - M_a (P / RT)}{M_a M_f (P / RT) - \rho} \quad (1)$$

Fuel-air mixing can be studied by mapping the combustor with a series of infinitesimal fluid elements and analyzing the evolution of mixture within each element using an Eulerian frame of reference. The evolutionary behavior of mixture can be studied using the logarithmic derivative of local equivalence ratio with respect to time,  $r_e(t)$ , which is given by<sup>15</sup>

$$r_e(t) = \frac{1}{\phi} \frac{d\phi}{dt} = \left( \frac{m_a}{m_f} \right)_{st} \frac{M_f}{M_a} (M_f - M_a) \frac{RT}{\phi} \times \left[ \left( P \frac{d\rho}{dt} - \rho \frac{dP}{dt} + \rho \frac{P}{T} \frac{dT}{dt} \right) / (M_f P - RT\rho)^2 \right] \quad (2)$$

Equation (2) shows that rates of equivalence ratio are linked to variations of pressure, temperature, and density. These variations are measured using total derivatives with respect to time. The total derivative of density with respect to time  $d\rho/dt$  will be called rate of density. In general, the rate of pressure depends on location and time and can be written as

$$\frac{dP}{dt} = \frac{\partial P}{\partial x} u + \frac{\partial P}{\partial y} v + \frac{\partial P}{\partial z} w + \frac{\partial P}{\partial t} \quad (3)$$

For steady-state conditions, Eq. (3) can be written as

$$\frac{dP}{dt} = \frac{\partial P}{\partial x} u + \frac{\partial P}{\partial y} v + \frac{\partial P}{\partial z} w$$

The rate of temperature can be determined in a similar manner. The equation of continuity<sup>6</sup> shows that the total derivative of fluid density with respect to time  $d\rho/dt$  is given by

$$\frac{d\rho}{dt} = -\rho \nabla \cdot (\mathbf{U}) \quad (4)$$

where  $\mathbf{U}$  is the overall velocity of flow. By definition, in Cartesian coordinates, the del vector operator  $\nabla$  is expressed as

$$\nabla = \mathbf{e}_1 \frac{\partial}{\partial x} + \mathbf{e}_2 \frac{\partial}{\partial y} + \mathbf{e}_3 \frac{\partial}{\partial z}$$

and the scalar product of the del operator  $\nabla$  and the velocity vector  $\mathbf{U}$ , i.e.,  $\nabla \cdot (\mathbf{U}) = \text{div } \mathbf{U}$  is the divergence of overall velocity. Therefore, in Cartesian coordinates, the velocity divergence is given by

$$\text{div } \mathbf{U} = \frac{\partial u}{\partial x} + \frac{\partial v}{\partial y} + \frac{\partial w}{\partial z}$$

Using Eq. (4), the rate of equivalence ratio can be expressed as

$$r_e(t) = \left( \frac{m_a}{m_f} \right)_{\text{st}} \frac{M_f}{M_a} (M_a - M_f) \frac{RT}{\phi} \times \left[ \left( P \rho \nabla \cdot U + \rho \frac{dP}{dt} - \rho \frac{P}{T} \frac{dT}{dt} \right) / (M_f P - RT \rho)^2 \right] \quad (5)$$

The preceding rate of equivalence ratio can be used to study mixing under both reacting and nonreacting conditions, so long as the fluid elements contain trace amounts of combustion products.

For diffusion flames, the equivalence ratio at the inlet is either infinity (in the fuel flow), or zero (in the air flow). Two mixing mechanisms that can be distinguished are the penetration of air into the fuel flow and the dispersion of fuel into the surrounding air.<sup>15</sup> Each mixing mechanism can be characterized by the time required to yield a flammable mixture. The time associated with the first mechanism, i.e., the time required to reduce the local equivalence ratio from infinity to the upper flammability limit,<sup>6</sup> is defined as  $t_r$ . A negative rate of equivalence ratio is required for this process. The fuel-lean mixing time  $t_l$  is the time associated with the second mechanism, i.e., the time required to increase the local equivalence ratio from zero to the lower flammability limit. This type of mixing requires a positive rate of equivalence ratio.

Based on Eq. (2), it can be shown that  $\phi(t)$  obeys the following law:

$$\phi(t) = \phi(0) \exp \left[ \int_0^t r_e(\tau) d\tau \right] \quad (6)$$

For elements that have an initial equivalence ratio of zero,  $\phi(t)$  is determined by taking the limit of Eq. (6) when  $\phi(0)$  tends to zero. For elements that initially contained only fuel,  $\phi(t)$  is determined by taking the limit of Eq. (6) when  $\phi(0)$  tends to infinity.

Assume that for a range of operational conditions, the rate of equivalence ratio is always greater than a certain minimum value  $r_e^{(\min)}$ , i.e.,

$$r_e^{(\min)}(t) < r_e(t) \quad (7)$$

Further, assume  $\phi(0)$  is kept constant. At time  $t$ , the equivalence ratios  $\phi^{(\min)}(t)$  and  $\phi(t)$  provided by  $r_e^{(\min)}(t)$  and  $r_e(t)$ , respectively, are given by

$$\phi^{(\min)}(t) = \phi(0) \exp \left[ \int_0^t r_e^{(\min)}(\tau) d\tau \right] \quad (8)$$

$$\phi(t) = \phi(0) \exp \left[ \int_0^t r_e(\tau) d\tau \right] \quad (9)$$

From inequality (7),

$$\int_0^t r_e^{(\min)}(\tau) d\tau < \int_0^t r_e(\tau) d\tau$$

and therefore

$$\frac{\exp \left[ \int_0^t r_e^{(\min)}(\tau) d\tau \right]}{\exp \left[ \int_0^t r_e(\tau) d\tau \right]} < 1 \quad (10)$$

From Eqs. (8) and (9)

$$\frac{\phi^{(\min)}(t)}{\phi(t)} = \frac{\phi(0) \exp \left[ \int_0^t r_e^{(\min)}(\tau) d\tau \right]}{\phi(0) \exp \left[ \int_0^t r_e(\tau) d\tau \right]} \quad (11)$$

Calculating the limits of  $\phi^{(\min)}(t)/\phi(t)$  when  $\phi(0)$  tends to zero and infinity shows that

$$\frac{\phi^{(\min)}(t)}{\phi(t)} = \frac{\exp \left[ \int_0^t r_e^{(\min)}(\tau) d\tau \right]}{\exp \left[ \int_0^t r_e(\tau) d\tau \right]} < 1 \quad (12)$$

for any initial fluid composition.

To achieve ignition and flame propagation, the equivalence ratio has to be maintained between the fuel-lean and fuel-rich flammability limits, which for the case of a methane-air diffusion flame are 0.5 and 1.68, respectively.<sup>6</sup> Assume  $\phi(t)$  is equal to the lean flammability limit. Inequality (12) shows that at  $t$ , the mixture provided by  $r_e^{(\min)}(t)$  is not yet flammable. In other words, if  $t_l$  and  $t_l^{(\max)}$  are the fuel-lean mixing times provided by  $r_e(t)$  and  $r_e^{(\min)}(t)$ , respectively, then  $t_l^{(\max)}$  is the maximum fuel-lean mixing time, i.e.,

$$t_l < t_l^{(\max)} \quad (13)$$

In the fuel flow, mixing requires a negative rate of equivalence ratio. Similarly, assuming  $r_e(t) < r_e^{(\max)}(t)$  at any instant, then the fuel-rich mixing time  $t_r^{(\max)}$ , which is provided by  $r_e^{(\max)}(t)$ , is the maximum fuel-rich mixing time, i.e.,

$$t_r < t_r^{(\max)} \quad (14)$$

For known distributions of pressure, temperature, and velocity, fuel-air mixing can be studied using Eqs. (5) and (6). Because of the complexity of real flows, both the fuel-rich and fuel-lean mixing times have to be determined numerically. Nevertheless, inequality relation in Eqs. (13) and (14) show that the  $t_r^{(\max)}$  and  $t_l^{(\max)}$  mixing times can be determined analytically if the minimum and maximum rates of equivalence ratio, i.e.,  $r_e^{(\min)}(t)$  and  $r_e^{(\max)}(t)$ , respectively, obey simple laws.

From Eq. (1), the difference between the equivalence ratio at a given time  $t$ ,  $\phi(t)$ , and  $\phi(0)$  is

$$\phi(t) - \phi(0) = \left( \frac{m_a}{m_f} \right)_{\text{st}} \frac{M_f}{M_a} \left\{ \frac{\rho(t) - M_a[P(t)/RT(t)]}{M_f[P(t)/RT(t)] - \rho(t)} - \frac{\rho(0) - M_a[P(0)/RT(0)]}{M_f[P(0)/RT(0)] - \rho(0)} \right\} \quad (15)$$

When the evolutionary behavior of pressure, temperature, and density are known, Eq. (15) can be used to provide the maximum values of both fuel-rich and fuel-lean mixing times. Assume that fluid elements within the air flow are subject to positive velocity divergence, i.e.,  $\text{div } U > 0$ , cooling, i.e.,  $dT/dt < 0$ , and  $dP/dt$ , which is always greater than a certain limit,  $(dP/dt)_{\min} > 0$ . Also assume that fluid elements within the fuel flow are subjected to negative velocity divergence, i.e.,  $\text{div } U < 0$ , heating, (i.e.,  $dT/dt > 0$ ), and a negative rate of pressure  $dP/dt < (dP/dt)_{\max}$ . Under these conditions within the air flow,

$$r_e^{(\min)}(t) < r_e(t) \quad (16)$$

where

$$r_e^{(\min)}(t) = \left( \frac{m_a}{m_f} \right)_{\text{st}} \frac{M_f}{M_a} (M_a - M_f) \frac{RT\rho}{\phi} \times \left[ \left( \frac{dP}{dt} \right)_{\min} / (M_f P - RT\rho)^2 \right]$$

$$r_e(t) = \left( \frac{m_a}{m_f} \right)_{\text{st}} \frac{M_f}{M_a} (M_a - M_f) \frac{RT}{\phi} \times \left[ \left( P \rho \text{div } U + \rho \frac{dP}{dt} - \rho \frac{P}{T} \frac{dT}{dt} \right) / (M_f P - RT\rho)^2 \right]$$

and within the fuel flow

$$r_e^{(\max)}(t) > r_e(t) \quad (17)$$

where

$$r_e^{(\max)}(t) = \left( \frac{m_a}{m_f} \right)_{\text{st}} \frac{M_f}{M_a} (M_a - M_f) \frac{RT\rho}{\phi} \times \left[ \left( \frac{dP}{dt} \right)_{\text{max}} / (M_f P - RT\rho)^2 \right]$$

$$r_e(t) = \left( \frac{m_a}{m_f} \right)_{\text{st}} \frac{M_f}{M_a} (M_a - M_f) \frac{RT}{\phi}$$

$$\times \left[ \left( P\rho \operatorname{div} U + \rho \frac{dP}{dt} - \rho \frac{P}{T} \frac{dT}{dt} \right) / (M_f P - RT\rho)^2 \right]$$

Therefore,  $t_r^{(\max)}$  and  $t_l^{(\max)}$  are provided by  $r_e^{(\max)}$  and  $r_e^{(\min)}$ , respectively. Equation (15) shows that both maximum mixing times are given by

$$t = \frac{M(0)P(0)}{M_a \langle dP/dt \rangle} \left[ \frac{1 + \phi(t)(m_f/m_a)_{\text{st}}(M_a/M_f)}{1 + \phi(t)(m_f/m_a)_{\text{st}}} - \frac{1 + \phi(0)(m_f/m_a)_{\text{st}}(M_a/M_f)}{1 + \phi(0)(m_f/m_a)_{\text{st}}} \right] \quad (18)$$

where the average rate of pressure  $\langle dP/dt \rangle$  takes the values of  $(dP/dt)_{\text{max}}$  and  $(dP/dt)_{\text{min}}$  in the fuel flow and in the surrounding air, respectively.

The maximum fuel-rich mixing time is obtained by calculating the limit when the initial equivalence ratio tends to infinity and the final equivalence ratio is 1.68. For a methane-air mixture, the maximum fuel-lean mixing time is obtained by considering an initial equivalence ratio of zero and a final equivalence ratio of 0.5. Therefore, the expressions for the  $t_r^{(\max)}$  and  $t_f^{(\max)}$  mixing times are, respectively,

$$t_r^{(\max)} = \frac{P(0)M(0)}{M_a (dP/dt)_{\text{max}}} \left[ \frac{1 + \phi(t)(m_f/m_a)_{\text{st}}(M_a/M_f)}{1 + \phi(t)(m_f/m_a)_{\text{st}}} - \frac{M_f}{M_a} \right] \quad (19)$$

$$t_l^{(\max)} = \frac{P(0)M(0)}{M_a (dP/dt)_{\text{min}}} \left[ \frac{1 + \phi(t)(m_f/m_a)_{\text{st}}(M_a/M_f)}{1 + \phi(t)(m_f/m_a)_{\text{st}}} - 1 \right] \quad (20)$$

In a similar manner, assume a positive velocity divergence  $\operatorname{div} U$  and rate of pressure  $dP/dt$  and a negative rate of temperature  $dT/dt < (dT/dt)_{\text{max}}$  within the air flow. In the fuel flow, one can assume that  $\operatorname{div} U$  and  $dP/dt$  are negative, whereas  $dT/dt$  is greater than a certain minimum value  $(dT/dt)_{\text{min}} > 0$ . Under these conditions, both the maximum fuel-rich and fuel-lean mixing times are calculated from

$$t = \frac{T(0)M_a}{M(0)\langle dT/dt \rangle} \left[ \frac{1 + \phi(t)(m_f/m_a)_{\text{st}}}{1 + \phi(t)(m_f/m_a)_{\text{st}}(M_a/M_f)} - \frac{1 + \phi(0)(m_f/m_a)_{\text{st}}}{1 + \phi(0)(m_f/m_a)_{\text{st}}(M_a/M_f)} \right] \quad (21)$$

where the average rate of temperature  $\langle dT/dt \rangle$  equals  $(dT/dt)_{\text{min}}$  in the fuel flow and  $(dT/dt)_{\text{max}}$  in the surrounding air. The maximum fuel-rich and fuel-lean mixing times are

$$t_r^{(\max)} = \frac{T(0)M_a}{M(0)(dT/dt)_{\text{min}}} \left[ \frac{1 + \phi(t)(m_f/m_a)_{\text{st}}}{1 + \phi(t)(m_f/m_a)_{\text{st}}(M_a/M_f)} - \frac{M_f}{M_a} \right] \quad (22)$$

$$t_l^{(\max)} = \frac{T(0)M_a}{M(0)(dT/dt)_{\text{max}}} \left[ \frac{1 + \phi(t)(m_f/m_a)_{\text{st}}}{1 + \phi(t)(m_f/m_a)_{\text{st}}(M_a/M_f)} - 1 \right] \quad (23)$$

The maximum mixing times provided by velocity gradients can be determined using a similar procedure. Within the air flow, assume a positive rate of pressure and a negative rate of temperature. The velocity divergence  $\operatorname{div} U$  is assumed to be positive and greater than a certain limit  $(\operatorname{div} U)_{\text{min}}$ . Within the fuel flow, assume a negative rate of pressure and positive rate of temperature, while  $\operatorname{div} U$  obeys the constraint:

$$\operatorname{div} U < \operatorname{div} U_{\text{max}} < 0$$

Under these conditions, the maximum values of both fuel-rich and fuel-lean mixing time are calculated from

$$t = -\frac{M_a}{M(0)\langle \operatorname{div} U \rangle} \left[ \frac{1 + \phi(t)(m_f/m_a)_{\text{st}}}{1 + \phi(t)(m_f/m_a)_{\text{st}}(M_a/M_f)} - \frac{1 + \phi(0)(m_f/m_a)_{\text{st}}}{1 + \phi(0)(m_f/m_a)_{\text{st}}(M_a/M_f)} \right] \quad (24)$$

where the average velocity divergence  $\langle \operatorname{div} U \rangle$  takes the values of  $(\operatorname{div} U)_{\text{max}}$  and  $(\operatorname{div} U)_{\text{min}}$  in the fuel and the surrounding air flow, respectively.

As shown, the maximum fuel-rich mixing time is provided by taking the limit when the initial equivalence ratio tends to infinity and the final equivalence ratio is 1.68 and the fuel-lean mixing time is obtained considering an initial equivalence ratio of zero and a final equivalence ratio of 0.5. The fuel-rich mixing time produced by velocity divergence is given by

$$t_r^{(\max)} = \frac{M_a}{M(0)(\operatorname{div} U)_{\text{max}}} \left[ \frac{M_f}{M_a} - \frac{1 + \phi(t)(m_f/m_a)_{\text{st}}}{1 + \phi(t)(m_f/m_a)_{\text{st}}(M_a/M_f)} \right] \quad (25)$$

Under the preceding conditions, the maximum fuel-lean mixing time is:

$$t_l^{(\max)} = \frac{M_a}{M(0)(\operatorname{div} U)_{\text{min}}} \left[ 1 - \frac{1 + \phi(t)(m_f/m_a)_{\text{st}}}{1 + \phi(t)(m_f/m_a)_{\text{st}}(M_a/M_f)} \right] \quad (26)$$

#### IV. Model Validation

The calculated rates of equivalence ratio, based on the preceding model, have been compared with the available experimental data for methane-air diffusion flame<sup>16</sup> and nonreacting hydrogen-air mixtures.<sup>17</sup> The experimental data for methane-air flames includes mass fractions, pressure, temperature, and velocity.<sup>16</sup> No turbulence data are available for the flames.<sup>16</sup> Details of the experimental test and setup are given in Ref. 16. For hydrogen-air mixtures, the data by Takagi et al.<sup>17</sup> include turbulence intensity and average flow. Information on density was calculated based on the mass fractions of nitrogen, oxygen, and hydrogen.

The fuel used by Masri et al.<sup>16</sup> was not pure methane but a mixture of 90% methane and 10% combustion products (produced by burning  $C_2H_2$ ). The apparatus consisted of a centrally located circular fuel nozzle for methane surrounded by an annular nozzle for products of  $C_2H_2$  combustion. This fuel is then mixed with the surrounding combustion air by diffusion. This setup was selected to provide strong interaction between flow turbulence and flame and to provide conditions that can be described by parabolic equations.<sup>16</sup> The flame approached extinction with increase in fuel velocity. For the examined conditions, flame extinction occurs at an axial distance of about  $140R_n$  downstream from the burner exit. As expected, jet velocities lower than those required for extinction yield a turbulent diffusion flame. The reported experimental accuracy for temperature and mass fractions is  $\sim 5\%$  (Ref. 16).

For nonreacting mixtures the fuel was a mixture of  $H_2$  and  $N_2$  having a volume ratio of 1/ 0.68. The fuel inlet velocity for the two cases analyzed here was 20.4 and 55.7 m/s, respectively. The Reynolds numbers corresponding to these velocities are 4200 and 11000, respectively.<sup>17</sup> At inlet, air had a uniform velocity of 5.1 m/s. No information is given on the experimental accuracy of reported data. All studies were carried out at one atmosphere pressure. Both fuel and air were injected axially.

For fluid elements containing initially only air, the rate of equivalence ratio (based on the initial equivalence ratio) cannot be defined; see Eqs. (2) and (5). Instead, the average value of equivalence ratio is used. This average value  $\bar{\phi}$  is given by

$$\bar{\phi} \approx (\phi_{i+1} + \phi_i)/2$$

Therefore, the experimental rate of equivalence ratio is given by

$$r_e^{(exp)}(t) \approx \frac{1}{\bar{\phi}} \frac{\phi_{i+1} - \phi_i}{x_{ax,i+1} - x_{ax,i}} u_{cyl} \quad (27)$$

Similarly, the values of the rates of density and temperature and velocity divergence are calculated. Model rates are calculated using Eq. (5).

The ratio of two numbers  $A$  and  $B$  (having uncertainties of  $a$  and  $b$ , respectively) has an uncertainty given by<sup>18</sup>

$$\varepsilon_r = \pm[(a/A) + (b/B)] \quad (28)$$

The uncertainty of  $A + B$  is given by<sup>18</sup>

$$\varepsilon_r = \pm(a + b) \quad (29)$$

The uncertainty of equivalence ratio, estimated from the known accuracy of  $\sim \pm 5\%$  for the mass fractions of fuel and air, is estimated to be about  $\pm 10\%$ ; see Eq. (28). The uncertainty of spatial location is less than 1 mm,<sup>16</sup> which is negligible compared to the step size, i.e.,  $x_{ax,i+1} - x_{ax,i}$ . Usually either the initial value of local equivalence ratio  $\Phi_i$  is much greater than the final equivalence ratio  $\Phi_{i+1}$  or vice versa. Therefore, the uncertainty of the rate of equivalence ratio is  $\sim \pm 20\%$ ; see Eqs. (27–29). For hydrogen–air mixtures, data on accuracy of experimental rates are not reported.

The mixing model requires accurate information on either the distribution of overall velocity of flow or density. Equations (2) and (5) show that the model accuracy deteriorates because of inaccurate density or overall velocity data [as velocity and density fluctuations are linked; see Eq. (4)]. The uncertainty of model results is expected to be comparable with the level of turbulent velocity fluctuations. If velocity fluctuations are negligible (2% of overall flow velocity or less), negligible error occurs with the model results using average instead of overall velocity of flow.

The results presented here include both nominal values and associated uncertainties (represented by error bars). Figure 1 shows

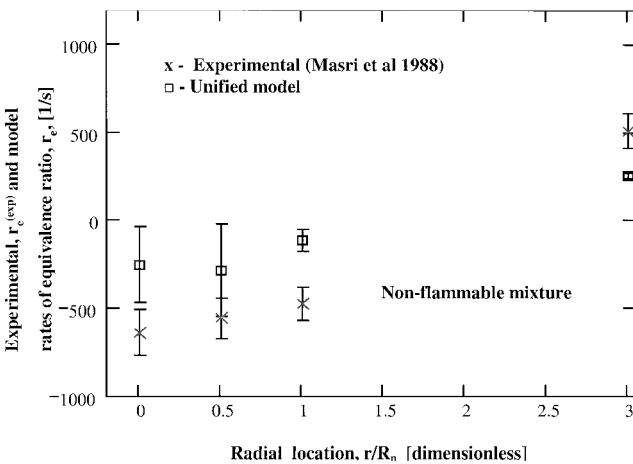


**Fig. 1** Comparison of the rates of equivalence ratio calculated from the mixing model and experimental data at an axial distance of  $x_{ax}/R_n = 40$  for methane–air flame having an initial fuel velocity of 41 m/s.

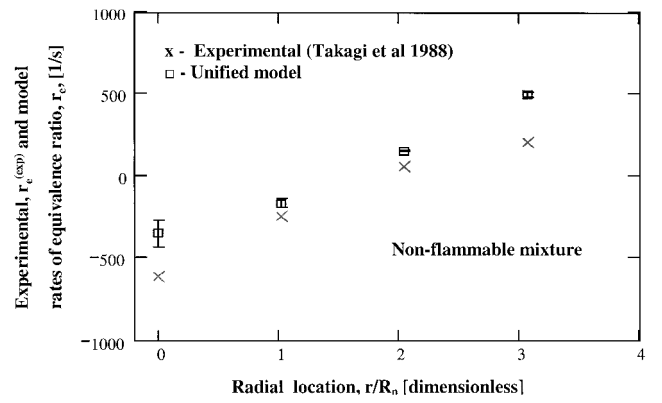


**Fig. 2** Comparison of the rates of equivalence ratio between the model results and experimental data<sup>17</sup> at an axial distance of  $x_{ax}/R_n = 12$  for  $Re = 4200$  for the nonreacting hydrogen–air mixture.

experimental  $r_e^{(exp)}$  and model  $r_e$ , rates of equivalence ratio for an initial fuel velocity of 41 m/s (for the diffusion flame  $L$ ), at an axial distance of  $x_{ax}/R_n = 40$  (a location where data are reported<sup>16</sup>). The Reynolds number is not specified. Both rates increase with radial distance, whereas the initial value of local equivalence ratio decreases from 142 to 0.587. Based on the reported data, the mixture<sup>16</sup> is nonflammable up to and including  $r/R_n = 3$  and flammable for  $4 > r/R_n > 3$ . It is to be noted that fuel was prepared by mixing methane with finite amount of  $C_2H_2$  combustion products (about 10% by mass). The accuracy of the finite difference scheme used to calculate the velocity divergence is reduced with increased density fluctuations. The data on turbulence are lacking. The level of turbulence is expected to increase near the flame front that will then result in less accurate model results. Therefore, the experimental and calculated rates cannot strictly be compared near to the axis of symmetry and in the vicinity of flame, i.e., at  $r/R_n = 0$  and  $r/R_n \geq 1$ . Otherwise the comparison shows good agreement.

The model and experimental rates of equivalence ratio for hydrogen–air mixtures at  $Re = 4200$  are shown in Fig. 2. The initial equivalence ratio ranged from 3.19 at  $r/R_n = 0$  to 3.2 at  $r/R_n = 5.2$ . The experimental accuracy is not provided and the step size is large (about 0.060 m) as compared to the flow. Both experimental and model rates of equivalence ratio increase with radial distance. At a radial distance of  $r/R_n = 0$ , the nominal values of experimental and model rates of equivalence ratio differ by up to 400 1/s. This difference is expected because of high turbulence levels and the fact that fuel is a mixture of hydrogen and nitrogen. For  $r/R_n = 1$  to 2, the ratio between oxygen and nitrogen within mixture is about 3.4 on a mass basis (a value close to that found for air) and velocity fluctuations are reduced to less than 10% of average velocity. As a consequence, the nominal rates of equivalence ratio differ by less than 100 1/s. For  $r/R_n = 3$ , the model rate is about two times greater than the experimental rate. This discrepancy can be attributed to increased turbulence levels. The largest differences between model and experimental results were observed for a Reynolds number of 11,000. For this case the level of velocity fluctuation exceeded 25% of average velocity.<sup>17</sup> As a consequence, model and experimental rates of equivalence ratio differ considerably. At locations where these velocities are comparable, i.e., for  $Re \leq 2100$ , and the mass fraction of fuel and air exceeds 90%, the model results are comparable with experimental data.

The model and experimental rates of equivalence ratio agree well for both methane–air mixtures under reacting conditions and hydrogen–air mixtures under nonreacting conditions. The model is therefore not limited to any specific fuel. The model can, therefore, provide accurate results at any turbulence levels with information on overall flow velocity.

## V. Model Accuracy and Applicability Limits

Model accuracy and applicability are limited by the assumptions made. Analyses of species concentration in combustors show that the ratio between oxygen and nitrogen remains constant outside

the flame. This reveals that by treating air as single specie during mixing causes negligible errors.<sup>6</sup> For pressures up to about 15 atm and temperatures exceeding 290 K the deviation from ideality is less than 3% (Ref. 19). Another source of error is from the assumption that no combustion products are present within the fluid element. If the mass fraction of products is less than 5%, Eq. (15) provides the final equivalence ratio with an accuracy of about 22%; see Eqs. (28) and (29). As a consequence, the uncertainty of fuel-lean and fuel-rich mixing times is less than 44%; see Eqs. (18–26). Additional errors can also arise because of uncertainties in the distribution of pressure, temperature, and overall velocity. These errors cannot be attributed to the model itself.

Assume that mixing is because of temperature gradients only and that the initial temperature of fuel and air exceeds 290 K and initial pressure is less than 10 atm. For any constant rate of temperature  $dT/dt$ , the final temperature attained during mixing with air penetrating into fuel is  $T(t_f) = T(0) + \langle dT/dt \rangle t_f = 1.68 T(0)$ ; see Eq. (21), where  $\langle dT/dt \rangle$  is the average rate of temperature over the mixing duration. Final temperature for the case of fuel dispersing into air is  $0.96 T(0)$ . Therefore, model accuracy does not degrade with rates of temperature. Similar analyses showed that rates of pressure and velocity divergence have negligible effect on model accuracy. As long as initial pressure remains less than 10 atm, initial temperature exceeds 290 K, and the mass fraction of combustion products present within the fluid element does not exceed 5%, the model uncertainty is less than 44%. The constraints on mass fraction of combustion products and initial pressure and temperature can be further relaxed at the expense of accuracy.

## VI. Computational Approach

The maximum mixing times for fuel-lean and fuel-rich limits in a nonreacting mixture have been calculated using MATHCAD 6.0. The results presented here show the time in which the equivalence ratio increases from zero to the lower flammability limit<sup>6</sup> (for the fuel-lean case) or the time required to reduce the equivalence ratio from infinity to the upper flammability limit (for the fuel-rich case). Because the mixing model used here is based on the ideal gas law, it cannot be used for mixtures having high density. This means that the results presented here are not valid only for high-pressure combustors. Distribution of pressure, temperature, and velocity divergence examined here are characteristic of low-pressure combustors. The initial pressure was varied from 1 to 5 atm. In the fuel flow,  $(dP/dt)_{\max}$ ,  $(dT/dt)_{\min}$ , and  $\text{div } \mathbf{U}_{\max}$  ranged from  $-1.1$  to  $0$  atm/s,  $0$  to  $1,500,000$  K/s and  $-150$  to  $0$  1/s, respectively. In the air flow,  $(dP/dt)_{\min}$ ,  $(dT/dt)_{\max}$ , and  $\text{div } \mathbf{U}_{\min}$  ranged from  $0$  to  $1.1$  atm/s,  $-1,500,000$  to  $0$  K/s, and  $0$  to  $150$  1/s, respectively. The range of velocity divergence and rate of temperature and pressure can be extended (see preceding section), if desired. In both fuel and air, the initial temperature ranged from 293 to 1465 K. In the fuel flow, the initial density varied from  $0.665$  to  $3.325$  kg/m<sup>3</sup>. In the air flow, the initial density was varied from  $1.2$  to  $6$  kg/m<sup>3</sup>.

## VII. Results and Discussion

Results presented here show the extent of mixing time variation as affected by the local values of initial pressure, temperature, rate of pressure, rate of temperature, and velocity divergence. The results are valid under both nonreacting and reacting conditions except when specified. For mixing times, a logarithmic scale is used to accommodate an extended range. Figure 3 shows the effect of pressure distribution on the maximum fuel-rich mixing time. Here, the fuel is subject to heating and a negative velocity divergence (which could be achieved by decelerating the fuel flow). An initial temperature of 293 K and an initial pressure in the range of 1 to 5 atm are considered. The densities corresponding to these pressures are  $0.665$  and  $3.326$  kg/m<sup>3</sup>, respectively. The results show that for rates of pressure having a magnitude of less than  $0.5$  atm/s and initial pressure of 5 atm or higher, the fuel-rich mixing time can exceed 4 s. If the rate of pressure tends to zero, the maximum fuel-rich mixing time tends to infinity and vice versa. For initial pressures of 1 and 5 atm and a rate of pressure,  $dP/dt < -1.1$  atm/s, the fuel-rich mixing times are less than 0.4 and 2 s, respectively. The maximum mixing time

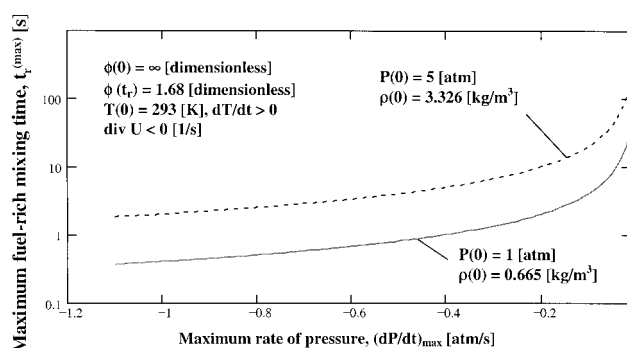


Fig. 3 Effect of pressure distribution on maximum mixing time for the case with air penetrating into the fuel flow.

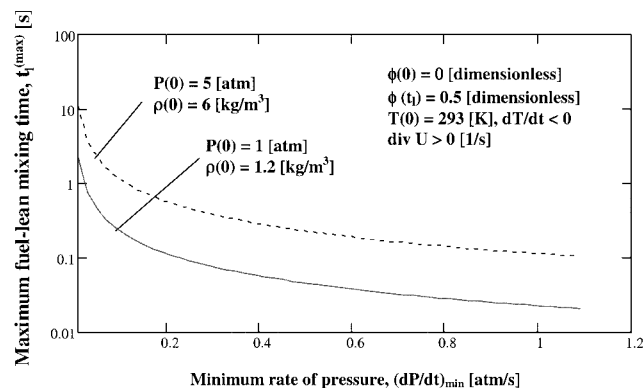


Fig. 4 Effect of pressure distribution on maximum mixing time for the case with fuel dispersing into the air flow.

is proportional to the pressure and inversely proportional to the rate of pressure; see Eq. (18). These results are in agreement with previous studies,<sup>15</sup> which showed that the rate of mixing is enhanced by reducing the initial pressure or increasing the rate of pressure.

The typical gas residence time ranges from a few milliseconds in gas turbine combustors to a few seconds in furnaces. Mixing due solely to a rate of pressure is too slow, unless the rate of pressure significantly exceeds 1 atm/s. For an initial pressure of 5 atm, the residence time would be insufficient to achieve complete mixing. Incomplete mixing leads to significant combustion inefficiency and yields large amounts of unburned hydrocarbon that may be released into the atmosphere. In furnaces where combustion takes place at atmospheric pressure, the slow mixing would produce a significant ignition delay.

The effect of pressure and rate of pressure on the maximum fuel-lean mixing time is shown in Fig. 4. An initial temperature of 293 K is considered here. Assume that the air flow is subjected to cooling and positive velocity divergence. The densities corresponding to the initial pressures of 1 and 5 atm are  $1.2$  and  $6.0$  kg/m<sup>3</sup>, respectively. For a rate of pressure exceeding  $1.1$  atm/s, the maximum fuel-lean mixing time is about  $0.02$  s when the initial pressure is 1 atm and  $0.3$  s when the initial pressure is 5 atm. Therefore, a lower initial pressure provides shorter mixing times for both cases of air or fuel dispersing into the other fluid. The maximum fuel-lean mixing time tends to infinity when the rate of pressure tends to zero and vice versa. This phenomenon is similar to the behavior of air penetrating the fuel flow. The maximum fuel-lean mixing time is also proportional to the initial pressure, as seen from Eq. (18). The results presented in Figs. 3 and 4 show that fuel dispersion into the surrounding air produces a flammable mixture about 20 times faster than air penetration into the fuel flow. The maximum fuel-rich and fuel-lean mixing times are inversely proportional to the rate of pressure. An increase in the rate of pressure provides progressively less effect on these mixing times. Simultaneous enhancement of both mixing mechanisms requires that the rate of pressure be positive in the air flow and negative in the fuel flow.

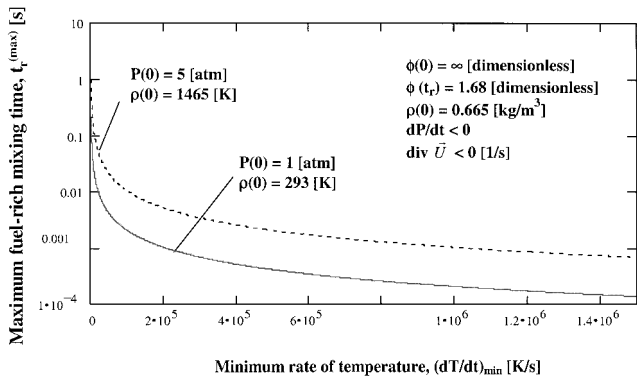


Fig. 5 Effect of temperature on the maximum mixing time for the case with air penetrating into the fuel flow.

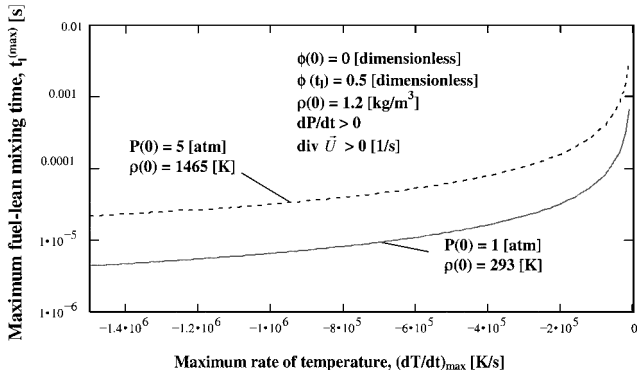


Fig. 6 Effect of temperature on the mixing time for the case with fuel dispersing into the air flow.

For mixing under nonreacting conditions, the rates of temperature (unless artificially enhanced) are negligible. Normally, the rates of temperature have a significant effect on mixing under reacting conditions. For rates of temperature exceeding 1,500,000 K/s, fuel-rich mixing times are less than 0.0002 s for an initial temperature of 293 K and less than 0.001 s for an initial temperature of 1465 K; see Fig. 5. The initial pressures that correspond to these temperatures are 1 and 5 atm, respectively. Negative rate of pressure and velocity divergence is considered. As the rate of temperature tends to zero the maximum fuel-rich mixing time tends to infinity and vice versa. Equation (22) shows that the maximum fuel-rich mixing time is proportional to the initial temperature and inversely proportional to the rate of temperature. These results are in agreement with previous studies<sup>15</sup> that showed a reduction in the rate of mixing at high temperatures and increase in the rate of mixing at high rates of temperature.<sup>15</sup> Rates of temperature of less than 1,000 K/s provide mixing times in excess of 0.3 s.

Figure 6 shows the affect of temperature on maximum fuel-lean mixing time. A constant density of 1.2 kg/m<sup>3</sup> and two initial temperatures of 293 and 1465 K, respectively, are considered here. The initial pressures that correspond to these temperatures are 1 and 5 atm, respectively. The rate of pressure and velocity divergence is assumed to be positive. For an initial temperature of 293 K, a rate of temperature of about -1,500,000 K/s provides a maximum fuel-lean mixing time of 6 μs. An initial temperature of 1465 K and a rate of temperature of -1,500,000 K/s provide a maximum fuel-lean mixing time of approximately 30 μs. For an initial temperature of up to 1465 K and a rate of temperature dT/dt > -1,000 K/s, maximum fuel-lean mixing time exceeds 0.005 s. The maximum fuel-lean mixing time is also proportional to the initial temperature and inversely proportional to the rate of temperature; see Eq. (23). As shown in Fig. 6, if air is cooled, the dispersion of fuel into the surrounding air is enhanced. For the range of temperatures and rates of temperature considered, the fuel-lean mixing time may be short enough to produce a flammable mixture in a few milliseconds, if air

could be cooled during mixing. Normally the temperatures of both air and fuel tend to increase because of the effect of flame.

Differences in heat capacity and distance to the flame may cause air and fuel to heat up at slightly different rates. Assuming that the initial temperatures of fuel and air are equal, any difference in temperature between these fluids, which may appear before the completion of mixing, will be slight. The effect of the strong heat flux provided by flame will prevail. The temperature of both fuel and air will increase continuously. As a consequence, mixing via air penetration into the fuel flow will be enhanced, although the dispersion of fuel into the surrounding air will be hampered. If the initial temperature of fuel and air are significantly different, one fluid may experience a brief period of cooling during mixing. If air is preheated, the air flow may cool during contact with fuel, but fuel temperature will increase not only from caloric radiation of flame but also by interaction with air. Under such conditions, both the dispersion of fuel into the surrounding air and the penetration of air into the fuel flow may contribute to mixing. In addition, higher initial temperature of air must be balanced by the high rate of cooling, otherwise the contribution of fuel dispersion into the surrounding air to mixing will be negligible. Fuel preheating may enhance combustion rates and contribute to mixing in flames. Nevertheless, in nonreacting mixtures, fuel preheating could reduce both mixing mechanisms. As a consequence, both the fuel-lean and the fuel-rich mixing times may increase.

Assuming an initial fuel temperature of less than 300 K, the fuel-rich mixing time can be reduced to a few milliseconds if the rate of temperature exceeds 10,000 K/s. If the initial temperature is 1465 K, the fuel-rich mixing time can be reduced to a few milliseconds only if the rate of temperature is greater than 50,000 K/s. The rate of temperature alone may not be sufficient to provide complete mixing. The preceding results have shown that rates of pressure and/or temperature alone may not assure complete mixing. Mixing has to be enhanced by another mechanism. As seen from Eq. (24), the maximum mixing times are inversely proportional to velocity divergence. High velocity divergence can significantly reduce both fuel-rich and fuel-lean mixing times. Figure 7 shows the effect of velocity divergence on both fuel-rich and fuel-lean maximum mixing times. Decreasing pressure is assumed within the fuel flow, i.e., dP/dt < 0, and increasing within the surrounding air, i.e., dP/dt > 0. Fuel is also subjected to heating, i.e., dT/dt > 0, whereas the surrounding air is cooled, i.e., dT/dt < 0. The left curve shows the effect of velocity divergence on the maximum fuel-rich mixing time whereas the right curve shows the effect on the maximum fuel-lean mixing time. An initial velocity divergence having a magnitude in excess of 50 s<sup>-1</sup> provides a maximum fuel-rich mixing time of less than 0.01 s. Velocity divergence that exceeds 50 s<sup>-1</sup> provides fuel-lean mixing times of less than 0.0005 s, even when acting alone, as shown in Fig. 7. For similar distributions of pressure, temperature, and velocity, the maximum fuel-rich mixing time is about 20 times larger than the fuel-lean mixing time. This is in agreement

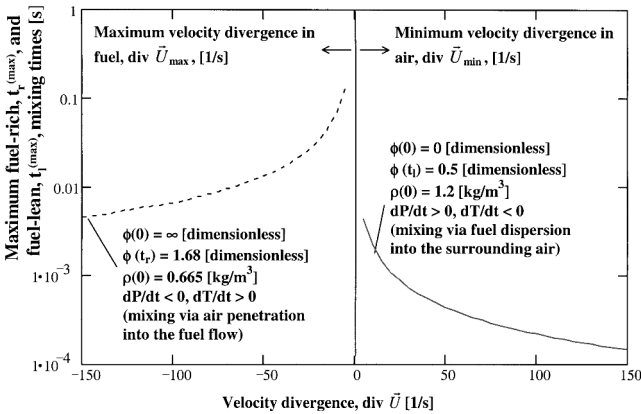


Fig. 7 Effect of velocity divergence on the maximum mixing time for the case of air penetrating the fuel flow and fuel dispersing the air flow.

with previous studies.<sup>15</sup> To achieve comparable fuel-rich and fuel-lean mixing times, the magnitude of the velocity divergence in the fuel flow should be about 20 greater than that in the air flow. Both maximum mixing times are inversely proportional to velocity divergence and tend to infinity when the velocity divergence tends to zero and vice versa. Temperature and velocity gradients are more effective for enhancing both mixing mechanisms than pressure gradients. The in-phase interaction of temperature and velocity gradients is required to assure enhanced mixing. Thus, to enhance mixing mechanisms the two combustor design guidelines that can be formulated are: 1) methane should be subjected to heating and negative velocity divergence, and 2) air should be subjected to cooling and positive velocity divergence. As a consequence, air preheating is recommended for methane-air flames. For similar distributions of pressure, temperature, and velocity, fuel-lean mixing times being shorter than fuel-rich mixing times, air penetration into fuel is the primary mixing mechanism. Therefore, a third combustor design guideline is the selection of air penetration into fuel when only one mechanism can be enhanced.

### VIII. Conclusions

The maximum mixing times are inversely proportional to constant rates of pressure, temperature, and density under both nonreacting and reacting conditions as long as the mixture does not ignite and contains only trace amounts of combustion products. At room temperature and in the presence of a rate of pressure no greater than 1.1 atm/s and negligible temperature and velocity gradients, more than 0.4 s are required to produce a flammable mixture. Under reacting conditions mixing takes place in the vicinity of flame, and the rate of temperature is positive in both the fuel flow and air flow. For this reason, the dispersion of methane gas into the surrounding air is reduced. Therefore, mixing proceeds better with air penetration into the fuel flow. The maximum mixing time is proportional to the initial temperature and inversely proportional to the rate of temperature. As a consequence, at higher initial temperature, the rate of temperature should be as high as possible to provide complete mixing in less than about a millisecond residence time available in gas turbine combustors. For the initial pressures and temperatures considered here, rapid and complete mixing, efficient combustion and low pollutants emission can be achieved by using large rates of density that are linked to high velocity gradients. To enhance both air penetration into the fuel flow and fuel dispersion into the surrounding air, velocity divergence should be negative in the fuel flow and positive in the air flow. For fuels that are lighter than air, preheating of the air assists in mixing.

### Acknowledgments

Partial support of this research by NASA Glenn Research Center, Department of Energy via the South Carolina Energy Research and

Development Center and the University of Maryland is gratefully acknowledged.

### References

- <sup>1</sup>Khavkin, Y. I., *Combustion System and Design*, Pennwell Books, Tulsa, OK, 1996, pp. xiii, xixi.
- <sup>2</sup>Gupta, A. K., and Lilley, D. G., "Combustion and Environmental Challenges for Gas Turbines in the 1990s," *Journal of Propulsion and Power*, Vol. 10, No. 2, 1994, pp. 137–147.
- <sup>3</sup>Beér, J. M., "Stationary Combustion, the Environmental Leitmotiv," *22nd Symposium (International) on Combustion*, The Combustion Institute, Pittsburgh, PA, 1988, pp. 1–16.
- <sup>4</sup>Cohen, H., Rogers, G. F. C., and Saravanamuttoo, H. I. N., *Gas Turbine Theory*, Wiley, New York, 1987, p. 24.
- <sup>5</sup>Someya, T. (ed.), *Advanced Combustion Science*, Springer-Verlag, Heidelberg, Germany, 1993, pp. 1–8.
- <sup>6</sup>Strehlow, R. A., *Combustion Fundamentals*, McGraw-Hill, New York, 1984, pp. 2, 28, 70–75, 114–120, 156–170, 242, 288–296, 353–373, and 484, 485.
- <sup>7</sup>Kuo, K. K., *Principles of Combustion*, Wiley, 1986, pp. 1, 2, 445, and 461.
- <sup>8</sup>Chomiak, J., *Combustion, A Study in Theory, Fact and Application*, Abacus Press, Gordon and Breach Science Publishers, New York, 1990, pp. 5, 336–350.
- <sup>9</sup>Harnby, M., Edwards, M. F., and Nienow, A. W., *Mixing in the Process Industries*, Butterworths, 1985, p. 174.
- <sup>10</sup>Rizk, N. K., and Mongia, H. C., "Gas Turbine Design Methodology," AIAA/ASME/SAE/ASME 22nd Joint Propulsion Conf., AIAA Paper 86-1513, Huntsville, AL, 16–18 June 1986.
- <sup>11</sup>Ottino, J. M., *The Kinematics of Mixing: Stretching, Chaos and Transport*, Cambridge Univ. Press, New York, 2nd edition, 1990, pp. 1–16.
- <sup>12</sup>Oldshue, J. Y., *Fluid Mixing Technology*, McGraw-Hill, New York, 1983, pp. 224–225, 229.
- <sup>13</sup>North, G. L., and Santavica, D. A., "The Fractal Nature of Premixed Turbulent Flames," *Combustion Science and Technology*, Vol. 72, 1990, pp. 215–232.
- <sup>14</sup>Guyon, E., Nadel, J. P., and Pomeaux, Y. (ed.), *Disorder and Mixing*, Klumer Academics Dordrecht/Boston/London, 1987, pp. 339–341.
- <sup>15</sup>Brasoveanu, D., and Gupta, A. K., "Analysis of Gaseous Fuel and Air Mixing," ASME Summer Fluids Engineering Meeting, Hilton Head, SC, 13–18 Aug. 1995; also Brasoveanu D., and Gupta, A. K., "Analysis of Gaseous Fuel and Air Mixing," *Combustion Science and Technology*, Vol. 141, 1999, pp. 111–121.
- <sup>16</sup>Masri, A. R., Bilger, R. W., and Dibble, R. W., "Turbulent Non-Premixed Flames of Methane Near Extinction: Probability Density Functions," *Combustion and Flame*, Vol. 73, No. 3, 1988, pp. 261–285.
- <sup>17</sup>Takagi, T., Shin, H. D., and Ishio, A., "Properties of Turbulence in Turbulent Diffusion Flames," *Combustion and Flame*, Vol. 40, 1981, pp. 121–140.
- <sup>18</sup>Scarborough, J. B., *Numerical Mathematical Analysis*, Johns Hopkins Press, Baltimore, 1962, pp. 4–18.
- <sup>19</sup>Hilsenrath, J., Beckett, C. W., Benedict, W. S., Fano, L., Hoge, H. J., Masi, J. F., Nuttall, R. L., Touloukian, Y. S., and Woolley, H. W., "Tables of Thermal Properties of Gases," *National Bureau of Standards, Circular*, Vol. 564, Nov. 1955, pp. 146–198, 313–368, 384–436, and 444–472.